Iraqi Journal of Science, 2026, Vol. 67, No. 6, pp: 3424-3436
DOI: 10.24996/ijs.2026.67.6.29

ISSN: 0067-2904

Photo-Thermal Conversion Properties of Selective Coatings with Aluminium and Nickel Powders Additives

Mustafa Ashoor Ryadh, Ahmed A. Al-Tabbakh*
Department of Physics, College of Science, Al-Nahrain University, Jadiriya, Baghdad, Iraq

Received: 25/11/2024 Accepted: 14/ 7/2025 Published: 30/6/2026

Abstract

Efficient solar energy harvesting through selective absorber coatings is critical for advancing sustainable thermal applications, such as domestic hot water production and water purification. Enhancing photo-thermal conversion while maintaining durability and ease of fabrication remains a challenge. To address this, a composite selective coating was developed by decorating a heat-resistant paint with aluminium and nickel particles, applied via air-spraying on the base paint layer. The coatings were characterized structurally, morphologically, and compositionally using optical microscopy, field-emission electron microscopy, UV-Vis spectroscopy, energy dispersive X-ray analysis, and elemental mapping. Photo-thermal conversion performance was evaluated by measuring solar absorbance and the maximum substrate temperature under solar irradiation using a flat-plate collector setup. The study correlates the photo-thermal conversion with the coatings' structural and compositional features. Notably, the coating decorated with nickel particles achieved a maximum solar absorbance of 96.07%, enabling substrate temperatures exceeding the boiling point of water without the need for antireflection coatings. The fabrication method and superior photo-thermal properties position this composite coating as a promising candidate for domestic hot water generation and water purification applications, outperforming conventional selective coatings regardless of collector geometry.

Keywords: Coating, Solar collectors, Photothermal effect, Optical absorption, Nanopowders.

خصائص التحويل الضوئي الحراري للطلاءات الانتقائية مع إضافات مساحيق الألومنيوم والنيكل

مصطفى عاشور رياض, أحمد عبدالرحمن احمد الطباخ
قسم الفيزياء, كلية العلوم, جامعة النهرين, الجادرية, بغداد, العراق

الخلاصة

يُعدّ الحصاد الفعّال للطاقة الشمسية من خلال طلاءات الامتصاص الانتقائية أمرًا بالغ الأهمية لتطوير التطبيقات الحرارية المستدامة، مثل إنتاج الماء الساخن المنزلي وتنقية المياه. ولا يزال تحسين التحويل الضوئي الحراري مع الحفاظ على المتانة وسهولة التصنيع يُشكّل تحديًا. ولمعالجة هذا التحدي، تم تطوير طلاء مركب انتقائي الامتصاص، وذلك باضافة جسيمات الالمنيوم والنيكل الميكروية الى طلاء مقاوم للحرارة عن طريق الرش الهوائي على طبقة الطلاء الأساسية. وتم فس هذا البحث توصيف الطلاءات هيكليًا

*Email: tabbakh2013@gmail.com

ومورفولوجياً وتركيبيًا باستخدام المجهر الضوئي، والمجهر الإلكتروني الماسح، ومطيافية الأشعة فوق البنفسجية والمرئية، وتحليل الأشعة السينية المشتتة للطاقة، ورسم الخرائط العنصرية. وتم تقييم أداء التحويل الضوئي الحراري للطلاءمن خلال قياس امتصاص الطاقة الشمسية وأقصى درجة حرارة للركيزة تحت الإشعاع الشمسي باستخدام جهاز تجميع الاشعاع الشمسي ذو اللوح المسطح. وتم الربط بين التحويل الضوئي الحراري والخصائص الهيكلية والتركيبية للطلاءات. تجدر الإشارة إلى أن الطلاء المُزخرف بجزيئات النيكل حقق امتصاصًا شمسيًا أقصى بنسبة 96.07%، مما أتاح درجات حرارة ركيزة تتجاوز درجة غليان الماء دون الحاجة إلى طلاءات مضادة للانعكاس. وتضع طريقة التصنيع وخصائصها الضوئية الحرارية المتفوقة هذا الطلاء المركب كمرشح واعد لتطبيقات توليد الماء الساخن المنزلي وتنقية المياه، متفوقًا على الطلاءات الانتقائية التقليدية بغض النظر عن هندسة المُجمّع.

1. Introduction

Photo-thermal conversion is a process of transforming light energy into heat [1]. The technology involved in this process is gaining attention for solar energy harvesting-related applications, such as water purification and thermoelectric power generation [2-5]. Developing efficient, cost-effective, and easily fabricated solar selective coatings offers significant advantages for addressing freshwater scarcity and enabling sustainable water heating and purification solutions [6, 7]. Increasing the photo-thermal conversion is essential for more efficient solar systems [8, 9]. This requires achieving two targets: increasing absorbance and minimising reflectance and emittance of the collector surface [10-12]. Achieving these goals requires different strategies because they depend on various ways to reach them. High-absorption surfaces are fabricated by specific engineering processes known as texturing, using black coating materials and multiple and composite coatings [13, 14]. The choice of the materials used is governed by the application requirements and the collector design. On the other hand, low emission properties are maintained using thin films of metals that reflect infrared radiation into the space where they are generated, leading to a reduction of heat losses. Additionally, anti-reflection coatings are used to reduce reflection and enhance light transmission [15].

In 2022, Kafle et al. explored the development of efficient and durable black nickel coatings for solar thermal collectors using the electrochemical bath method [16]. They succeeded in optimizing the electrochemical synthesis of the coatings by controlling the pH level, temperature, electric current density and deposition time. These parameters were linked to the structural and optical properties and photothermal conversion characteristics of the coating. They identified the optimal parameters of the synthesis method that led to the best conversion characteristics. Reyna et al. synthesized and characterized nickel–cobalt mixed metal oxides for use as selective coatings in flat-plate solar collectors [10]. They used a nitrate decomposition reaction to synthesize the oxides and characterized them using various techniques like XRD, Raman spectroscopy, and SEM-EDS. The coatings were tested in a domestic flat solar collector, showing outstanding performance under real operating conditions. The investigated nickel–cobalt mixed oxides exhibited high solar absorbance of 94% and good thermal stability. In 2024, Junli et al. demonstrated the development of a single-layered cermet absorber with a structure of Ti@a-C cermet layer/a-C protective layer/SiO_2 antireflective layer [17]. This absorber was found to achieve absorption of 96.5% of the incident radiation in the UV, visible, and near-infrared bands. To further enhance absorption, a quasi-optical micro cavity structure based on cermet-metal-cermet was proposed. With such a structure, an absorption rate of 97.1% was achievable. The absorbers exhibited high thermal stability, maintaining performance after annealing at various temperatures. The absorbers were highly efficient in practical scenarios, insensitive to

incident angle and polarization state, and might be fabricated using a simple, lithography-free method. These results pave the way for large-area applications of a-C matrix materials, offering a sustainable solution for efficient solar energy utilization.

The key criteria of electromagnetic radiation absorption by matter are the following [18, 19]: Interaction mechanism, which involves the nature of interaction between the radiation and matter. Electromagnetic radiation in the ultra-violet and visible regions interacts with the electrons, leading to their excitation to higher energy levels. Infrared radiation affects the vibrational states of the molecular bonds of the materials. This means that the type of materials present in the coating determines the amount of radiation to be absorbed. Energy matching, which entails that absorption occurs if the energy difference between two quantized energy states of the absorbing material exactly matches the wavelength of the incident radiation. This means that each wavelength is absorbed by a specific material. Accordingly, each material has its‒absorption spectrum. The concentration of the absorbing material affects the absorption characteristic. This means that the surface density of the powders affects the surface absorptivity.

In the present work, enhancement of the photo-thermal conversion was attempted by increasing the absorption characteristics of a composite coating applied on aluminium substrates. The composite coating was prepared by adding aluminium or nickel metal powders on top of a black coating layer. The morphological properties and photo-thermal conversion behaviour were measured and discussed. The thermal conversions of the coating were compared with those investigated by other researchers using different composite coatings. Suggestions for further research are presented at the end of the discussion.

2. Materials and Methods

The substrates used in the present work were a 1 mm-thick aluminium plate of 95% purity purchasd from the local market. The substrates were cut into 4 cm×4 cm square pieces. Each substrate was subjected to systematic cleaning to remove unwanted impurities such as dirt, oil, and grease. The cleaning procedure started with mechanical polishing of the surfaces, followed by thorough washing with distilled water and acetone. The final step of cleaning was air drying. All substrates were coated with a heat-resistant black paint, known as Rust-Oleum V2100 System Enamel aerosols from Rust-Oleum Corporation/USA, which is commercially available on the market. This paint has a mat black appearance, high adhesion and anti-crack characteristics, a reasonably short curing time, and is resistance to moderately high temperatures. The photo-thermal conversion characteristics of the heat-resistant paint were investigated and reported in earlier work [20]. Aluminium or nickel metal powders were air-sprayed on top of the primary coating immediately after its application to the substrate surface. Despite being less quantifiable than other methods, this method guarantees adequate distribution homogeneity. It is also expected to allow for a homogeneous diffusion of the metal powder particles used to enhance the coating characteristics for the solar-to-thermal conversion application. The coating thickness was measured using an LS220 coating thickness gauge manufactured by Shenzhen Linshang Technology, China. Once the coating thickness is measured, its gravimetric density can be determined from the coating surface area.

The coated substrates were investigated primarily under an LED light source optical microscope from CoolingTech, China. The coating morphology was then examined under a scanning electron microscope. The elemental analysis and elemental distribution of the composite coatings were determined by electron energy dispersive spectroscopy (EDS) using

XFlash-6l10 detector from Bruker attached to the scanning electron microscope. The UV-Vis spectroscopy was used to determine the spectral reflectance of the coatings. Radiosity, is defined as the total radiant flux leaving a surface per unit area, was measured for the current coatings using a Pyrheliometer-like setup (see reference [20] for a detailed description of the measurement setup). Radiosity involves measuring the emitted, reflected and transmitted components of radiation expressed in units of W/m^2. Finally, the photo-thermal conversion was investigated using a flat-plate solar collector. The substrate temperature was measured with exposure time to solar radiation.

3. Results and Discussion

Figure 1 shows the substrates under the optical microscope. Figure 1 (a) shows the uncoated aluminium substrate in which longitudinal and unidirectional grooves are observable. These were due to brush cleaning performed on the substrate. These grooves ensured the required adhesion of the primary coating on the Al substrate, after which they became less visible as they were filled with the primary coating. The addition of the metal powders on top of the primary coating was evident from the optical microscope images (Figure 1 (b) and (c)). The distribution feature of the particles is believed to be a direct result of the spraying process adopted in the present work.

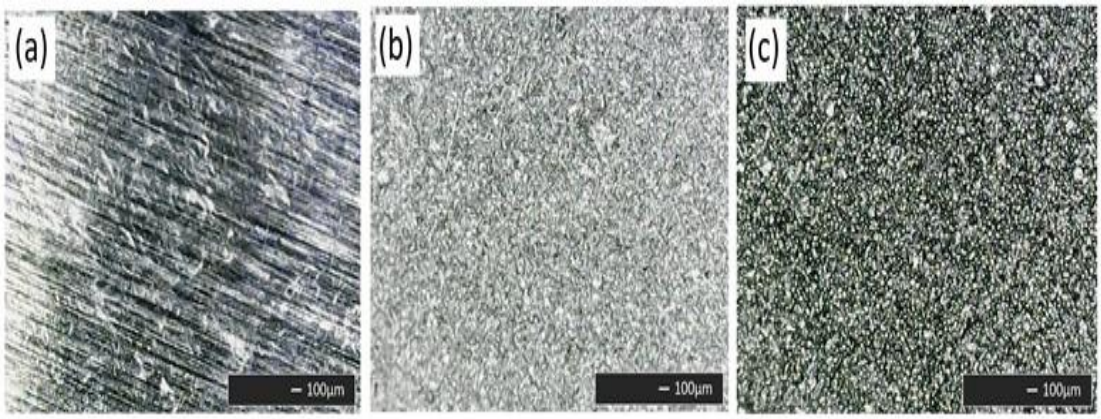

Figure 1: The aluminium substrates under optical microscope. (a) uncoated substrate (b) Heat-Resistant Paint (HRP) decorated with Al particles (c) HPR decorated with Ni Particles.

The surface morphology of the composite coatings was investigated using an Inspect S50 scanning electron microscope (SEM) from FEI, Netherlands. Figure 2 shows low and high-resolution micrographs of the Al/HRP and Ni/HRP composite coatings. Careful inspection of the SEM images confirms that the spraying process led to homogeneous coverage of the primary coating surface with the metal powders. Both composite coatings exhibited rough surface morphologies attributed to the deposition of particulate additives of the metal powders onto the primary coating layer. Scanning electron microscopy revealed distinct microstructural features for each formulation. For aluminium-incorporated coating, uniformly distributed particles with sizes ranging from 10 - 50 µm were observed. The nickel-incorporated coating featured hierarchally structured clusters (~60 µm in diameter) composed of finer secondary agglomerates (1-3 µm particle size). These clusters were evenly dispersed across the coating surface, forming a homogeneous distribution of micro-scale features. The nickel powder coating showed a unique structure of tiny, round-shaped clusters submerged in the paint matrix. Each cluster was made of several nanoparticles that agglomerate to form bigger particles. These clusters were attached, forming a complex rough morphology, which is believed to assist the harvesting of the incident radiation because the surface is rich with

many cavities that may assist the multiple internal reflections of the incident radiation rays. Such property is essential in the photo-thermal conversion character of the coating. These morphologies are associated with the photo-conversion efficiency of the coating. The complex rough morphology of the coating surface increases the effective surface area with which the incident radiation interacts, causing an increase in the photo-thermal conversion. These features are believed to play an important role in the sought functional behaviour of the coatings because the particles are expected to act as centres for selective absorption of the incident electromagnetic radiation. Furthermore, the spaces and gaps between the particles may act as trapping centres for the incident light. This may eventually enhance the absorption of the incident solar radiation via scattering and multiple reflections [21, 22]. Furthermore, the complex morphology with protruding asperities might be more reactive to the indirect components of the incident radiation (i.e. the diffused radiation). The most effective situation is when the solar radiation falls perpendicularly on the collector surface. Thus, the protruding features (providing segments of the area not parallel to the whole coating surface) allow the indirect radiation to fulfil the perpendicular incidence on the collector surface. This also allows the incident radiation with the chance to penetrate deeper inside the absorbing surface.

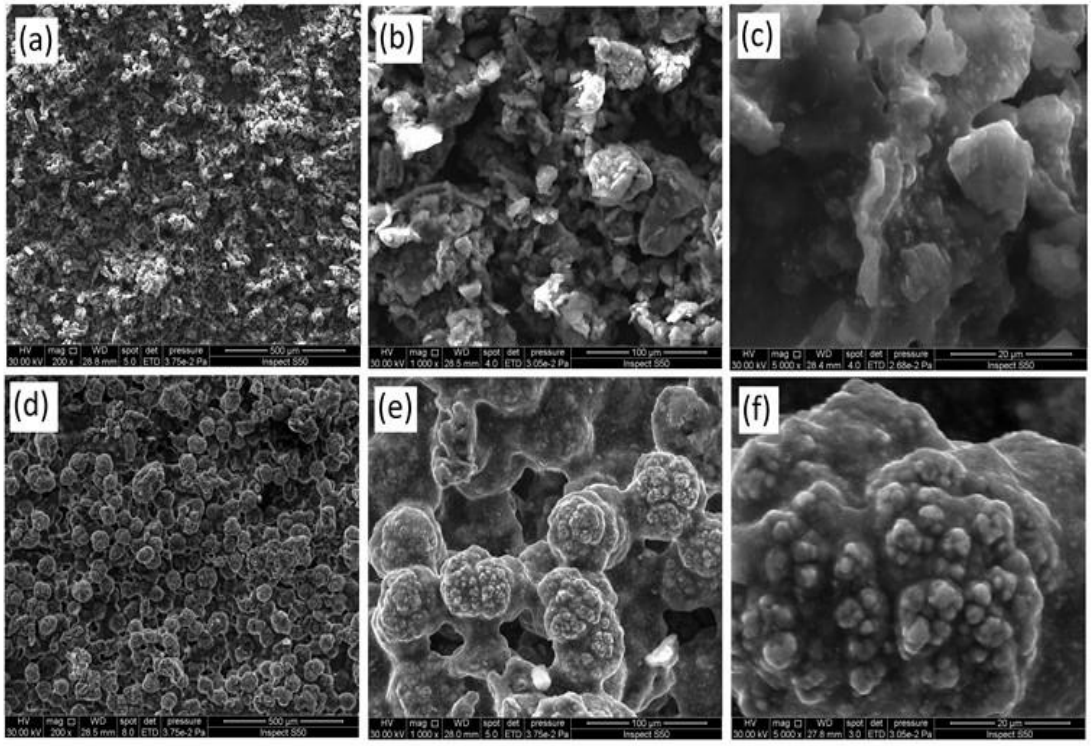

Figure 2: The scanning electron micrographs of the composite coatings. (a-c) low and high magnification images of Al/HRP coating. (d-f) low and high magnification images of Ni/HRP coating.

The EDS spectra and the elemental mapping of the Al/HRP and Ni/ HRP are shown in Figures 3 and 4, respectively. The peak height in the EDS spectrum correlates with the concentration of the element identified. The relative height of two peaks on the same EDS spectrum may also be used to compare the elemental concentration of the respective elements within the material under investigation. The element concentrations are tabulated and demonstrated below the EDS spectra. The elemental mapping of the three most occurring elements is shown under each spectrum. Silicon, chromium and ferrite are the elements present in the prepared coating because the primary paint (the heat-resistant black paint) is synthesized from silicon-modified alkyd resin and chromium and ferrite-based pigments.

Other elements are due to some contamination during specimen preparation. The elements identified were obtained based on Mosely's law. A comparison of the peak position of each element identified in the EDS spectra confirms this. For example, peaks due to the presence of silicon appear at an energy of 1.739 keV, aluminium at 1.486 keV, iron at 6.398 keV and Nickel at 7.471 keV. The peak positions of these elements are characteristic of their respective elements and are determined and identified from the characteristic X-ray emissions at equivalent energies [23].

The spectral reflectance of the composite coatings was measured in the ultra-violet-visible range (i.e. 200 – 1000 nm). All the spectra showed common or comparable characteristics of two distinct peaks (see Figure 5). These peaks were at wavelength values at which the intensity of the incident light signal is mostly reflected from the coating surfaces. The intensities of the peaks and peak positions vary with the addition of different powders to the heat-resistant paint. Also, the peak intensity and position vary depending on particle size, oxidation state, and local environment. The area under the curves was determined to be 8.48 a.u. and 3.29 a.u. for the Al and Ni-containing coatings, respectively. As the area under the curve increases, the coating has high reflectivity, hence low absorbance towards the incident radiation. This behaviour will facilitate a qualitative comparison of the coatings' absorptivity and support the findings from total reflection measurements (Table 1). Accordingly, the Ni/HRP coating has higher absorbance than the Al/HRP coating. For the uncoated substrate, it is well-known that the aluminium surface is known to have high UV-Vis reflectance, making it suitable for various optical applications. However, surface morphology and inertness (ex., presence of an oxide layer) can affect the reflective properties of the surface. Uncoated aluminium exhibits high reflectance across a broad spectrum. UV-Vis spectra showed distinct peaks related to reflectance higher than 90% at 248 nm, 400 nm and 532 nm. An unprotected oxidized aluminium surface exhibited a drop in the reflectance to about 50 – 60 % [27]. Nickel particles and their oxides show absorption features near visible wavelengths, likely due to excitation of surface vibrations [24–26]. The reflectance peaks around 600 nm, observed in Figure 5, align well with the known optical properties of nickel particles. These peaks probably arise because the metal particles act as scattering centers, enhancing light trapping and thus increasing absorption in the coating. In contrast, these peaks were less pronounced when aluminium particles were added to the coating.

The spectral characteristics are not the only decisive parameters as far as the photo-thermal conversion is concerned. Other factors are important, such as the surface morphology and the presence of certain surface features that may act as multiple reflections and trapping centres for the incident radiation. Thermal conductivity may also play an important role in the photo-thermal conversion character of the composite coating. The photo-thermal conversion was investigated directly by measuring the substrate temperature due to exposure to solar radiation.

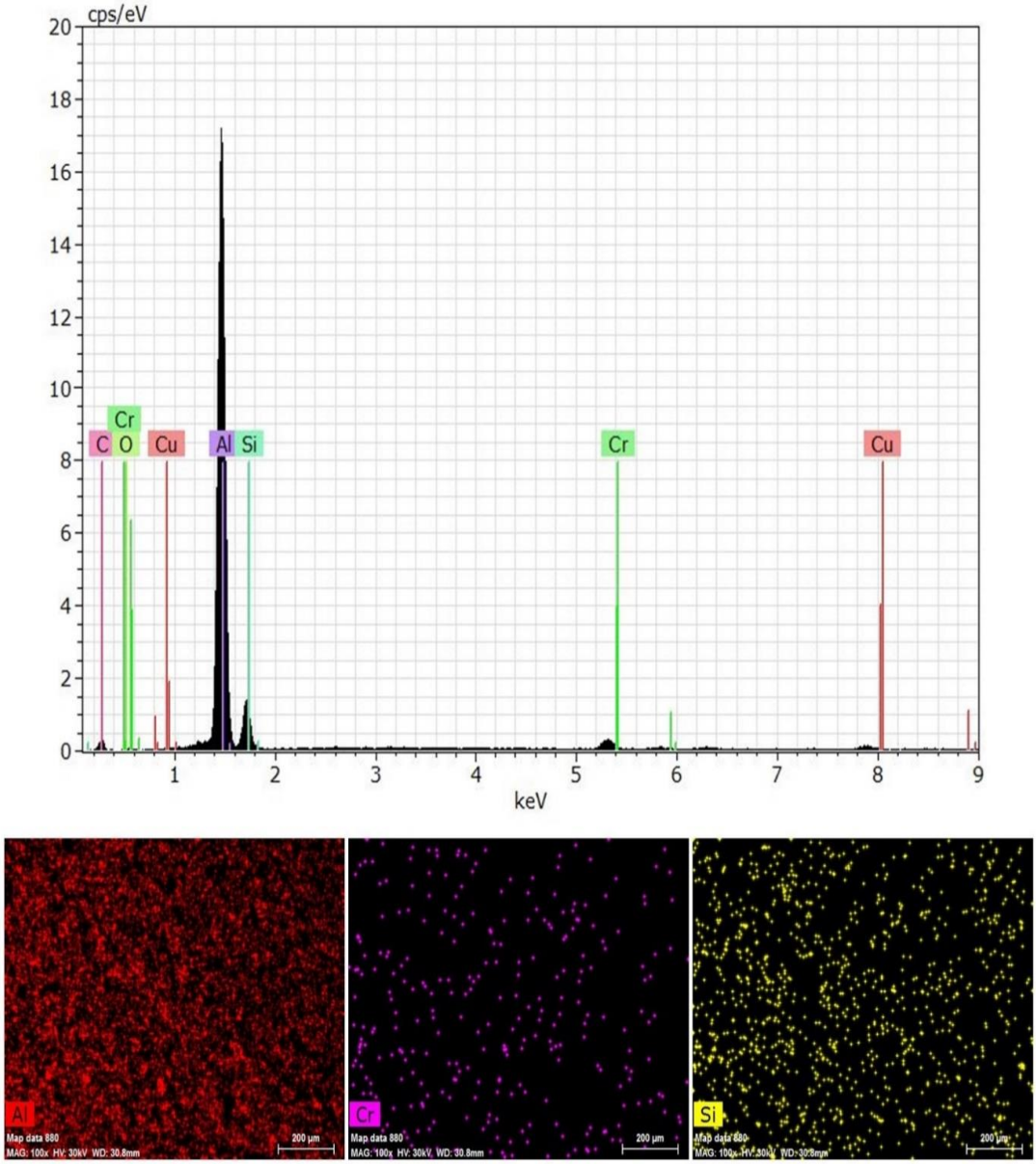

El	AN	Series	unn. C [wt.%]	norm. C [wt.%]	Atom. C [at.%]	Error (1 Sigma) [wt.%]
Al	13	K-series	58.58	63.58	46.38	3.01
C	6	K-series	28.21	30.62	50.18	8.86
Si	14	K-series	2.29	2.48	0.27	0.15
O	8	K-series	2.06	2.24	2.75	1.31
Cr	24	K-series	0.99	1.08	0.41	0.08
		Total:	92.13	100.00	100.00	

Figure 3: The elemental analysis and elemental mapping of the Al/HRP composite coating by EDS analyzer.

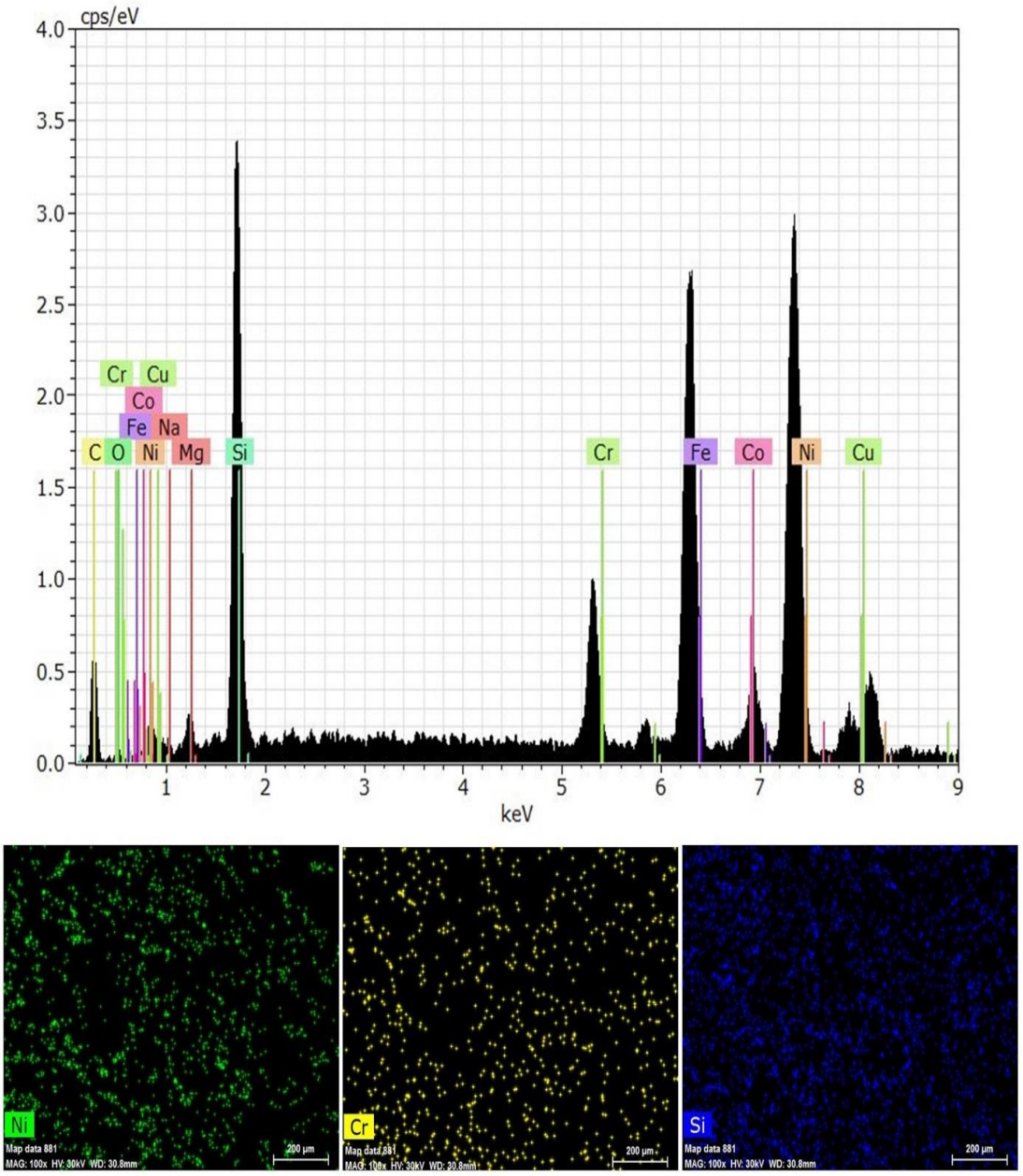

El	AN	Series	unn. C [wt.%]	norm. C [wt.%]	Atom. C [at.%]	Error (1 Sigma) [wt.%]
C	6	K-series	15.09	34.56	73.22	4.48
Ni	28	K-series	8.07	18.48	8.01	0.31
Si	14	K-series	7.38	16.89	2.38	0.33
Fe	26	K-series	7.24	16.58	7.56	0.28
Co	27	K-series	2.33	5.33	2.30	0.14
Cr	24	K-series	2.24	5.14	2.51	0.13
Na	11	K-series	0.70	1.60	1.77	0.16
O	8	K-series	0.62	1.42	2.25	0.59
		Total:	43.67	100.00	100.00	

Figure 4: The elemental analysis and elemental mapping of the Ni/HRP composite coating by EDS analyzer.

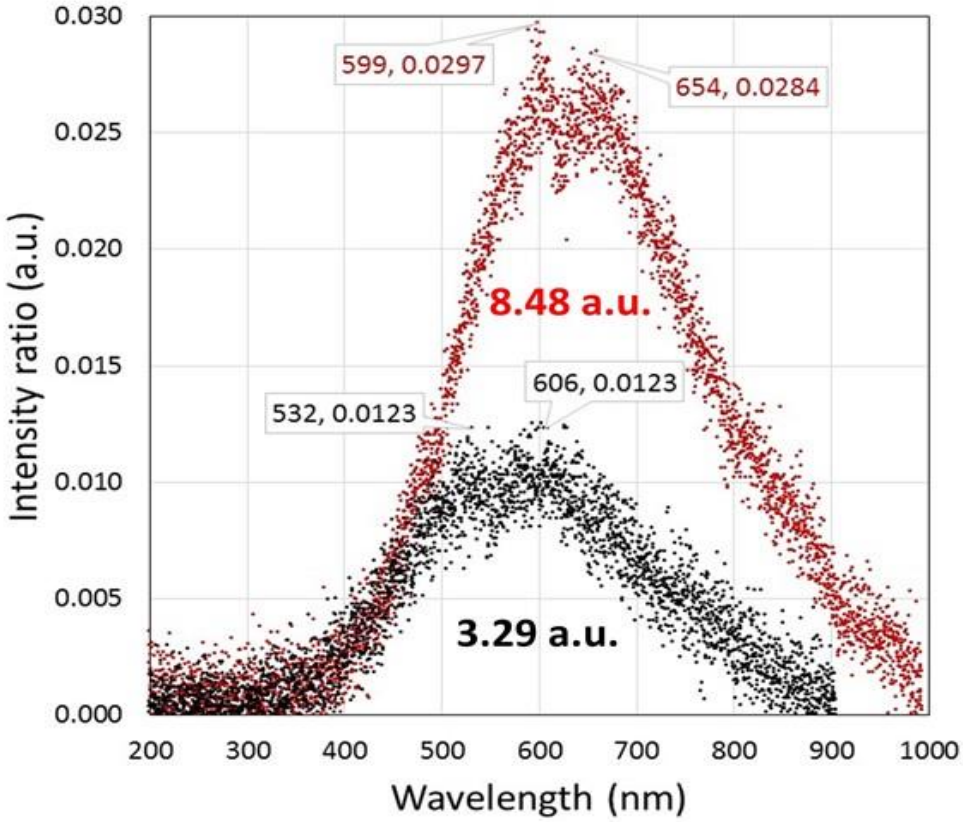

Figure 5: The UV-Vis reflectance spectra of the Al/HRP(red-coloured spectrum) and Ni/HRP(black-coloured spectrum) composite coatings.

The total reflection of the incident radiation was measured via a homemade pyrheliometer-like setup. A detailed description of the device setup was reported by Jasim and Al-Tabbakh [20]. The device setup allows for estimating the total reflected radiation in relation to the incident radiation after the exclusion of the diffused radiation. The absorbance values were then determined from the corresponding reflected intensities. Table 1 lists the absorbance of all the substrates. The Ni/HRP showed an absorbance of 96.07% at incident radiation of 1122 w/m^2; the Al/HRP coating exhibited an absorbance of 95.63%. Both composite coatings showed enhanced absorbance compared with the HRP-coated substrate. These results agree generally with the areas under the curve values of the UV-Vis spectra.

Table 1: The absorptivity of the composite coatings as determined from the reflected radiation.

Coating	Irradiance (W/m^2)	Reflected Intensity (W/m^2)	Absorbance (%)
Uncoated Al-substrate	1186	760	35.91
HRP	1186	67	94.32
Al / HRP	1100	48	95.63
Ni/HRP	1122	44	96.07

The photo-thermal conversion of the coatings was measured using the flat-plate collector setup. The temperature of the substrate is recorded against the time of exposure to solar radiation. The measurement continues until a maximum temperature is reached. At this temperature, the substrate is under thermal equilibrium. This means that the energy absorbed by the specimen is equal to the energy lost. Figure 6 shows the photo-thermal conversion

curves of the coatings. The substrate temperature increased rapidly immediately after exposure to solar radiation. Then, a saturation behaviour was observed as the substrate temperature reached its maximum value. The maximum temperatures of the substrates are listed in Table 2. The thickness and density of the composite coatings were also determined and tabulated. As the maximum temperature of the uncoated substrate reached 350.75 K (77.6 °C) at 1176 W/m^2, the Al/HRP and Ni/HRP coatings achieved 361.95 K (88.8 °C) and 375.5 K (102.4 °C), respectively. This might be attributed to multiple effects. Our results showed that the Ni/HRP coating had a higher thickness and density. The Ni/HRP-coated substrate was exposed to slightly higher irradiance. The complexity of surface morphology plays an important role in the absorbance characteristic of the surface. The type, distribution and concentration of the coating constituting elements are also essential in determining the coating photo-thermal conversion capacity. The morphology and structural aspects are expected to improve the surface's photo-thermal conversion due to the increase in multiple reflections and enhancement of surface absorbance at a wide range of solar radiation incidences on the coating surfaces.

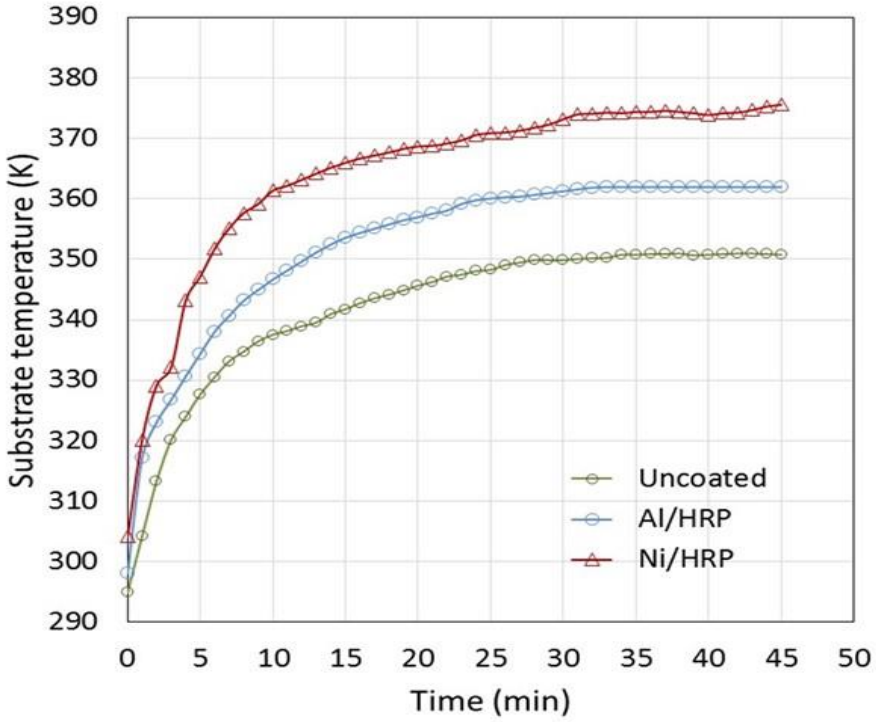

Figure 6: The photo-thermal conversion curves of the uncoated and coated substrates.

Table 2: The maximum substrate temperature

Coating	Thickness (μm)	Density (g/cm^3)	Irradiance (W/m^2)	$T_{max.}$ (°C)
Uncoated substrate	NA	2.7	1176	77.6
Al/HRP	71	0.615	1121	88.8
Ni/HRP	929	0.888	1131	102.4

The decoration of heat-resistant paint with aluminium and nickel particles enhanced the coating's photo-thermal conversion performance. The morphological, structural, and compositional aspects of the composite coating decide its photo-thermal conversion character. There are also other possibilities for the enhancement of the photo-thermal conversion of the coating, like adding an antireflection coating layer and mixing Al and Ni powders in an optimal ratio. Such approaches will be investigated in future work. In

comparison with other composite coatings, as shown in Table 3, the present investigated coatings showed greater photo-thermal conversion. Table 3 also exhibits a comparison of the photo-thermal conversion in terms of the substrate temperature. The Al/HRP and Ni/HRP composite coatings could lead to higher substrate temperature as compared with the CNT-CuO nanoparticles dispersed in black paint, CuO nanoparticles in black paint and NiAl alloy embedded in black paint. However, future research may be directed to incorporating other materials in the composite coating, such as metal-organic frameworks and plasmonic metal nanoparticles, which could lead to broadband solar absorption and conversion efficiency while maintaining durability of coatings.

Table 3: Comparison of the substrate maximum temperature for different coatings.

Coating Type	Irradiance (W/m^2)	$T_{substrate}$ (°C)	Reference
Al/HRP	1121	101.7	Present work
Ni/HRP	1131	102.4	Present work
CNT-CuO NPs dispersed in black paint	964	84.3	[28]
CuO NPs mixed with black paint	1100	97	[29]
NiAl Alloy embedded in black paint	1000	69.7	[30]

4. Conclusions

The photo-thermal conversion of a heat-resistant paint was enhanced successfully by adding metallic particles of aluminium and nickel powders on the top of the coating base layer. The submerged particles resulted in complex structural and morphological features that play a critical role in the photo-thermal conversion characteristics of the coating. This has been attributed to the enhancement of the surface absorbance to the incident radiation and the contribution of surface morphological features in trapping the incident radiation. The absorbance values of the Al and Ni decorated coatings were 95.63 % and 96.07%, respectively. The maximum temperature of the substrate was higher than the boiling temperature of water, making these composite coatings suitable for many domestic applications. The coating could easily be prepared and applied irrespective of the substrate geometry. The photo-thermal conversion of the composite coating is superior to many conventional alternatives, making it a suitable candidate for flat-plate and trough collectors.

Disclosure and Conflict of Interest

The authors declare that they have no conflicts of interest.

References

[1] A. Rojas, R.C. García-Zuñiga, A. Colin-Vidal, U. Nogal, J. Hernández Wong, M. Aguilar-Frutis, R.A. Muñoz-Hernández, E. Marín and A. Calderón, "Photothermal conversion for the solar energy use," *Latin American Journal of Physics Education*, vol. 17, no. 1, pp. 1-7, 2023.

[2] A. Shaik, R. J. Anandhi, S. Navdeep, P. Ashish, S. Nitin, Q. Mohammad, "Comprehensive Review on Low-Cost, Solar-Powered Water Purification Technologies for Remote Areas," *E3S Web of Conferences*, vol. 505, no. 02005, pp. 1-9, 2024. https://doi.org/10.1051/e3sconf/202450502005.

[3] A. Aziz, S. A. A. Shah, A. Hussain, S. T. Alam, M. Islam, M. Ur-Rehman, "Solar-Driven Advancements for Water Purification: Harnessing Sustainable Energy for Potable Water Provisioning," *Journal of Xi'an Shiyou University, Natural Science Edition*, vol. 19, no. 8, pp. 583-591, 2023.

[4] D. Edyta, F.-K. Natalia, "Hybrid Domestic HotWater System Performance in Industrial Hall," *Resources*, vol. 9, no. 65, pp. 1-12, 2020. https://doi.org/10.3390/resources9060065.

[5] B. F. Nicanor, A. C. Reymart, S. R. Neil Francis, G. R. Rhoda Jane, "Thermoelectric Generator: A Source of Renewable Energy," *Indonesian Journal of Energy*, vol. 3, no. 1, pp. 1–11, 2020. https://doi.org/10.33116/ije.v3i1.47.

[6] S.M. Shalaby, Mohamed E. Zayed, Farid A. Hammad, Ahmed S. Menesy, Ayman Refat Abd Elbar, "Recent Advances in Membrane Distillation Hybrids for Energy-Efficient Process Configurations: Technology Categorization, Operational Parameters Identification, and Energy Recovery Strategies," *Process Safety and Environmental Protection*, vol. 190, part A, pp. 817-838, 2024. https://doi.org/10.1016/j.psep.2024.07.098

[7] Mohamed E. Zayed, Ammar H. Elsheikh, F.A. Essa, Ahmed Mohamed Elbanna, Wenjia Li, Jun Zhao, "Chapter 12—High-temperature solar selective absorbing coatings for concentrated solar power systems. In Sustainable Materials and Green Processing for Energy Conversion," Editors: Cheong, K.Y., Apblett, A., Elsevier: Amsterdam, The Netherlands, 2022; pp. 361–398. https://doi.org/10.3390/app14188438.

[8] S. Khamlich, F. Ismail, M. W. Schouw, O. Nemraoui, "Photo Thermal Conversion Efficiency of Spectrally Selective Cr2o3/Cr/Cr2o3 Multilayered Solar Absorber," *AIUE Proceedings of the 18th Industrial and Commercial Use of Energy Conference* 2020.

[9] L. Qichen and W. Xun, "Recent Progress of Sub-Nanometric Materials in Photothermal Energy Conversion," *Advances in Science*, vol. 9, p. 2104225, 2022. https://doi.org/10.1002/advs.202104225.

[10] B. M. D. Reyna, M. H. Z. Dallely, A. S. Manuel, G,-V. Octavio, P. F. B. Adriana, R. G. Geonel, A. R.-G. Miguel, "Enhanced Performance of Nickel–Cobalt Oxides as Selective Coatings for Flat-Plate Solar Thermal Collector Applications," *Coatings*, vol. 13, no. 1329, pp. 1-18, 2023. https://doi.org/10.3390/coatings13081329.

[11] D. Chun, Y. Ziyi, M. Anzhen, D. Xuanming, Y. Guowei, "Self-enhancing photothermal conversion of 2D Weyl semimetal WTe2 with topological surface states for efficient solar vapor generation," *Nano Research*, vol. 6, pp. 10976–10984, 2023. https://doi.org/10.1007/s12274-023-5852-2.

[12] W. Laura, E. M. Jonathan, B. Helen, "The Far-Infra-Red Spectrometer for Surface Emissivity (FINESSE) – Part 2: First measurements of the emissivity of water in the far-infrared," *Atmospheric Measurement Techniques*, vol. 17, pp. 4777–4787, 2024. https://doi.org/10.5194/amt-17-4777-2024.

[13] C. Huige, S. Run, Z. Tierui, "Nanostructured Photothermal Materials for Environmental and Catalytic Applications," *Molecules*, vol. 26, no. 7552, pp. 1-20, 2021. https://doi.org/10.3390/molecules26247552.

[14] C. Ximin, R. Qifeng, Z. Xiaolu, X. Xinyue, H. Jingtian, F. Runfang, L. Yang, W. Jianfang, and X. Hongxing, "Photothermal Nanomaterials: A Powerful Light-to-Heat Converter," *Chemical Reviews*, vol. 123, no. 11, pp. 6891-6952, 2023. https://doi.org/10.1021/acs.chemrev.3c00159.

[15] F. Michael, "Types of Anti-Reflective Treatments and When to Use Them," *The Photonics Solutions Update*, pp. 28-31, 2024. www.photonicsonline.com

[16] B. P. Kafle, Bijaya Basnet, Bikash Timalsina, Akash Deo, Tek N. Malla, Nayan Acharya and A. Adhikari,"Optical, structural and thermal performances of black nickel selective coatings for solar thermal collectors," *Solar Energy*, vol. 234, pp. 262–274, 2022. https://doi.org/10.1016/j.solener.2022.01.042.

[17] S. Junli, C. Gang, L. Dingquan, M. Chong, X. Ping, Z. Sheng, W. Shuguang, L. Xingyu, L. Haihan, "Novel Ultrathin Quasi-Optical Microcavity-Selective Absorber Based on Ti@a‑C Cermet for Solar-Thermal Conversion," *ACS Photonics*, vol. 11, pp. 2637-2649, 2024. https://doi.org/10.1021/acsphotonics.4c00329.

[18] L. He, J. Hongwei, Z. Ke and J. Z. Zhiqiang, "Analysis of factors influencing actual absorption of solar energy by building walls," *Energy,* vol. 215(B), p. 118988, 2021. https://doi.org/10.1016/j.energy.2020.118988.

[19] H. Fouzi, H. Mustapha, R. Khadidja, Z. Katir, "Selective Surfaces for Photo-Thermal Conversion for Medium Solar Temperature Applications," *International Journal of Heat and Technology*, vol. 40, no. 1, pp. 219-224, 2022. https://doi.org/10.18280/ijht.400126.

[20] R. H. Jasim and A. A. Al-Tabbakh, "Enhancement of the Solar-Thermal Response of Flat-plate Collector Coated with a Heat-resistant Paint," *Jordan Journal of Physics*, vol. 15, no. 3, pp. 323-329, 2022. https://doi.org/10.47011/15.3.10.

[21] Z. Xie, H. Wang, M. Li, Y. Tian, Q. Deng, R. Chen, X. Zhu and Q. Liao, "Photothermal trap with multi-scale micro-nano hierarchical structure enhances light absorption and promote photothermal anti-icing/deicing," *Chemical Engineering Journal*, vol. 435, no. 3, p. 135025, 2022. https://doi.org/10.1016/j.cej.2022.135025.

[22] O. A. Charles, J. M. Robinson, A. O. Alex, O. A. Benard, M. M. Boniface, K. J. Pushpendra, "Controlled Texturing of Aluminum Sheet for Solar Energy Applications," *Advances in Materials Physics and Chemistry*, vol. 5, pp. 458-466, 2015. http://dx.doi.org/10.4236/ampc.2015.511046.

[23] S. Tomas, M. F. Lorcan, E. Waleed, "One hundred years of Moseley's law: An undergraduate experiment with relativistic effects", *American Journal of Physics*, vol. 85, no. 5, pp. 352-358, 2017. http://dx.doi.org/10.1119/1.4977793.

[24] Q. M. Salman, "Spectroscopic study of UV-VIS electronic transitions of Ni2+ ions in different phases of Sol- Gel process", *Journal University of Kerbala*, vol. 14, no. 4, pp. 34-43, 2016.

[25] A. M. Sadaa, Z. T. Al Abdullah, "Green Synthesis of Nickel Nanoparticles and their Application of Removal of Aliphatic Hydrocarbons from Crude Oil," *Iraqi Journal of Science*, vol.62, no.11, pp. 4333-4341, 2021. http://dx.doi.org/10.24996/ijs.2021.62.11(SI).14.

[26] M. Hemalatha, N. Suryanarayanan, S. Prabahar, "Synthesis and characterization of nickel nanoparticles by chemical reduction method," *Optoelectronics and Advanced Materials*, vol. 8, no. 3-4, pp. 288 – 291, 2014.

[27] O. Stenzel, S. Wilbrandt, J.-Y. He, S. Stempfhuber, S. Schröder and A. Tünnermann, "A Model Surface for Calculating the Reflectance of Smooth and Rough Aluminum Layers in the Vacuum Ultraviolet Spectral Range," *Coatings*, vol. 13, no. 1, p. 122, 2023. https://doi.org/10.3390/coatings13010122.

[28] T. K. Abdelkader, Y. Zhang, E. S. Gaballah, S. Wang, Q. Wan, Q. Fan, "Energy and Exergy Analysis of a Flat-Plate Solar Air Heater Artificially Roughened and Coated with a Novel Solar Selective Coating," *Journal of Cleaner Production*, vol. 250, p. 119501, 2019. https://doi.org/10.1016/j.jclepro.2019.119501.

[29] S. Sivakumar, C. Velmurugan, D. S. Ebenezer Jacob Dhas, A. Brusly Solomon and K. Leo Dev Wins, "Effect of nano cupric oxide coating on the forced convection performance of a mixed-mode flat plate solar dryer," *Renewable Energy*, vol. 155, pp. 1165-1172, 2020. https://doi.org/10.1016/j.renene.2020.04.027.

[30] E. Al-Shamaileh, "Testing of a new solar coating for solar water heating applications," *Solar Energy*, vol. 84, no. 9, pp. 1637-1643, 2010. https://doi.org/10.1016/j.solener.2010.06.003